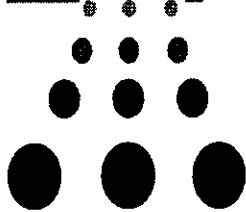




Jefferson Lab PAC14 Proposal Cover Sheet



This document must be received by close of business Thursday, **June 4, 1998** at:

Jefferson Lab
User Liaison Office,
Mail Stop 12B
12000 Jefferson Avenue
Newport News, VA
23606

Experimental Hall: A
Days Requested for Approval: 15

- New Proposal Title:** *Measurement of $P(\bar{e}, e, p)$ and the Strangeness Content of the Proton*
 - Update Experiment Number:**
 - Letter-of-Intent Title:**
- (Choose one)

Proposal Physics Goals

Indicate any experiments that have physics goals similar to those in your proposal.

Approved, Conditionally Approved, and/or Deferred Experiment(s) or proposals:

Approved E93-022

Conditionally approved: PR97-005

Contact Person

Name: *Haiyan Gao*

Institution: *MIT*

Address: *26-413 MIT*

Address: *77 Mass. Ave*

City, State, ZIP/Country: *Cambridge, MA 02139*

Phone: *(617) 258-0256*

Fax: *(617) 258-5440*

E-Mail: *haiyan@mit.lns.mit.edu*

Jefferson Lab Use Only

Receipt Date: 6/4/98

PR 98-103

By: ga

LAB RESOURCES LIST

JLab Proposal No.: 98-103
(For JLab ULO use only.)

Date 6/4/98

List below significant resources — both equipment and human — that you are requesting from Jefferson Lab in support of mounting and executing the proposed experiment. Do not include items that will be routinely supplied to all running experiments such as the base equipment for the hall and technical support for routine operation, installation, and maintenance.

Major Installations *(either your equip. or new equip. requested from JLab)*

New Support Structures: _____

Data Acquisition/Reduction

Computing Resources: _____

New Software: _____

Major Equipment

Magnets: _____

Power Supplies: _____

Targets: LHz target

Detectors: _____

Electronics: _____

Computer Hardware: _____

Other: _____

Other: _____

HAZARD IDENTIFICATION CHECKLIST

JLab Proposal No.: 98-103
(For CEBAF User Liaison Office use only.)

Date: 6/4/98

Check all items for which there is an anticipated need.

<p>Cryogenics</p> <p><input checked="" type="checkbox"/> beamline magnets <input type="checkbox"/> analysis magnets <input type="checkbox"/> target type: _____ flow rate: _____ capacity: _____</p>	<p>Electrical Equipment</p> <p>_____ cryo/electrical devices _____ capacitor banks _____ high voltage _____ exposed equipment</p>	<p>Radioactive/Hazardous Materials</p> <p>List any radioactive or hazardous/toxic materials planned for use:</p> <p>_____</p> <p>_____</p> <p>_____</p>
<p>Pressure Vessels</p> <p>_____ inside diameter _____ operating pressure _____ window material _____ window thickness</p>	<p>Flammable Gas or Liquids</p> <p>type: _____ flow rate: _____ capacity: _____</p> <p>Drift Chambers</p> <p>type: _____ flow rate: _____ capacity: _____</p>	<p>Other Target Materials</p> <p>_____ Beryllium (Be) _____ Lithium (Li) _____ Mercury (Hg) _____ Lead (Pb) _____ Tungsten (W) _____ Uranium (U) _____ Other (list below)</p> <p>_____</p> <p>_____</p>
<p>Vacuum Vessels</p> <p>_____ inside diameter _____ operating pressure _____ window material _____ window thickness</p>	<p>Radioactive Sources</p> <p>_____ permanent installation _____ temporary use</p> <p>type: _____ strength: _____</p>	<p>Large Mech. Structure/System</p> <p>_____ lifting devices _____ motion controllers _____ scaffolding or _____ elevated platforms</p>
<p>Lasers</p> <p>type: _____ wattage: _____ class: _____</p> <p>Installation:</p> <p>_____ permanent _____ temporary</p> <p>Use:</p> <p>_____ calibration _____ alignment</p>	<p>Hazardous Materials</p> <p>_____ cyanide plating materials _____ scintillation oil (from) _____ PCBs _____ methane _____ TMAE _____ TEA _____ photographic developers _____ other (list below)</p> <p>_____</p> <p>_____</p>	<p>General:</p> <p>Experiment Class:</p> <p><input checked="" type="checkbox"/> Base Equipment _____ Temp. Mod. to Base Equip. _____ Permanent Mod. to Base Equipment _____ Major New Apparatus</p> <p>Other: _____</p> <p>_____</p>

Measurement of $p(\vec{e}, e'\vec{p})\phi$ and the Strangeness Content of the Proton

A. Bernstein, T. Black, W. Bertozzi, C. Crawford, T.W. Donnelly, K. Fissum
H. Gao (spokesperson), S. Gilad, S. Jeschonnek, M. Pavan, D. Rowntree, W. Turchinets,
C. Williamson, F. Xiong, Wang Xu, J. Zhao, Z.L. Zhou
Massachusetts Institute of Technology

C. Glashausser, R. Gilman, X. Jiang, G. Kumbartzki, J. McIntyre,
R.D. Ransome (spokesperson), S. Strauch
Rutgers University

J.R. Calarco (spokesperson), F.W. Hersman, M. Holtrop, M.B. Leuschner
University of New Hampshire

T.-S.H. Lee
Argonne National Laboratory

W. Boeglin, L. Kramer, P. Markowitz, B. Raue
Florida International University

A.I. Titov
Joint Institute for Nuclear Research, Russia

T. Morii
Kobe University, Japan

S.N. Yang
National Taiwan University, Taiwan

Y. Oh
Seoul National University, Korea

L. Auerbach, Z.-E. Meziani, K. Slifer
Temple University

J.P. Chen, K. de Jager, E. Chudakov, J. Gomez, J.-O. Hansen, M. Kuss,
J. LeRose, M. Liang, R. Michaels, A. Saha, B. Wojtsekhowski
Thomas Jefferson National Accelerator Facility

D. Dale, W. Korsch
University of Kentucky

E.J. Beise, J.J. Kelly, P.G. Roos
University of Maryland

and the Hall A Collaboration

Abstract

The strange quark content of the nucleon is one of the most important questions in medium energy physics. Recent calculations show that some of the double polarization observables in the photoproduction and electroproduction of a ϕ meson from a proton target are extremely sensitive to the strange quark content of the proton. We propose to measure the polarization of the recoil proton from electroproduction of the ϕ mesons with a longitudinally polarized electron beam and a liquid hydrogen target. The scattered electrons and recoil protons will be detected in coincidence and ϕ mesons will be identified by missing mass reconstruction. We propose to make measurement on the $p(\vec{e}, e'\vec{p})\phi$ at a fixed invariant mass of 2.15 GeV and at $|Q^2| = 0.135 \text{ (GeV/c)}^2$. The time requested for this experiment is 15 days.

I. INTRODUCTION

In the naive constituent quark model, which has been quite successful in its description of the low lying states of the baryon [1], the nucleon ground state is composed of three valence quarks, two with flavor up and one with flavor down in the proton, and *vice-versa* in the neutron.

However, in a more realistic description of the nucleon, the three valence quarks are surrounded by quark-antiquark pairs which fluctuate out of the vacuum, the so-called “sea” quarks. The sea is often assumed to be symmetric in the three light quark flavors. However, because the s quark is heavier, this symmetry may be broken. Since the up and down quarks are the lightest and, hence, have the longest fluctuation lifetimes, most of the sea is likely to consist of $u\bar{u}$ and $d\bar{d}$ pairs. Nevertheless, although strange quarks are heavier and thus $s\bar{s}$ pairs would have a lower probability of being in the sea at a given time, they are expected to be there at some level.

This picture of $s\bar{s}$ pairs in the quark sea has been used to explain a number of experimental observations. These include (1) an anomalous value for the σ term observed in πN scattering, (2) deviations of the nucleon spin structure functions integrated over Bjorken x from theoretical predictions, as observed in the deep inelastic scattering (DIS) of polarized leptons from polarized nucleons, (3) a larger than expected value of the proton axial-vector form factor observed in νp scattering, and (4) a much larger than expected cross section ratio $p\bar{p} \rightarrow \phi\pi^+\pi^-/p\bar{p} \rightarrow \omega\pi^+\pi^-$.

Low energy theorems relate the isospin even π - N scattering amplitude $\Sigma = F_\pi^2 \bar{D}^+(2m_\pi^2)$, which is determined by extrapolating πN scattering to the unphysical pion pole [2], to the σ term $\sigma = \langle p|(m_u + m_d)(u\bar{u} + d\bar{d})|p\rangle/4M_N$. Naive estimates based on the baryon mass spectrum give $\sigma \approx 25 \text{ MeV}$. However, analysis of the πN scattering experiments gives $\Sigma \approx 60 \text{ MeV}$ (Koch gives a value of $64 \pm 8 \text{ MeV}$ [3]). This discrepancy and its possible interpretation in terms of strange quarks in the nucleon was first addressed by Cheng and Dashen [4]. Subsequently, the results have been analyzed and interpreted as evidence for $s\bar{s}$ in the nucleon quark sea. Gasser *et al.* extract a value [5]:

$$\langle p|s\bar{s}|p\rangle/\langle p|u\bar{u} + d\bar{d}|p\rangle \sim 0.1$$

indicating about a 10% admixture of strange quarks.

Most of the focus on the issue of strange quarks in the proton has arisen from the results of a series of experiments on the Deep Inelastic Scattering (DIS) of leptons on nucleons. Polarized DIS measurements on the proton were pioneered at SLAC [6]. The so-called “spin crisis” originated from the DIS of polarized muons on polarized protons performed by the European Muon Collaboration (EMC) [7], combined with the earlier SLAC measurements. These experiments measured the spin structure function of the proton $g_1^p(x)$ over a wide range of Bjorken variable x , particularly trying to extend the measurements to small x . By extrapolating to $x = 0$, EMC obtained $\int_0^1 dx g_1^p = \Gamma_1^p = 0.114 \pm 0.012 \pm 0.026$ (where the errors are, in order, statistical and systematic as is usually quoted) in disagreement with the sum rule of Ellis and Jaffe [8]. They had predicted a value of 0.189 ± 0.005 based on the best available values for the axial-vector and vector coupling constants G_A and G_V from neutron beta decay and the $SU(3)$ coupling constants F and D from hyperon beta-decay *and* assuming that the strange quark contribution to the nucleon spin was $\Delta s = 0$. Analysis of the data [7] indicated that only about 14% of the nucleon spin is due to the spin of the quarks with the remainder due to gluons and/or orbital angular momentum. If the discrepancy is assumed to be due to $s\bar{s}$ pairs in the quark sea, then they account for about 20% of the nucleon spin and in the opposite direction to the u and d contributions, mostly canceling them *i.e.* $\Delta s \approx -0.1$.

The discrepancy with the Ellis-Jaffe sum rule prompted further experiments by SMC [9] and SLAC E142 [10] and E143 [11]. These efforts, together with later measurements on the neutron by the SLAC E154 [12] and HERMES collaborations [13], which gave $\Gamma_1^n = -0.036 \pm 0.004 \pm 0.005$, confirmed the agreement with the Bjorken sum rule and the discrepancy with that of Ellis and Jaffe. The most recent analyses now give the net valence quark contribution to the proton spin as $\Delta q \approx 0.33$ and the strange sea quark contribution as $\Delta s \approx -0.10$ [14]. Additional measurements on $g_1^p(x)$ and $g_1^n(x)$ to even lower x have recently been made by SLAC E155 and HERMES but are as yet unpublished. Thus, the extracted value of the strange quark contribution to the proton spin has remained remarkably robust through these measurements. However, the method of determining this value, which has also been consistent, is model dependent.

Measurement of the cross section for νp elastic scattering was used by Ahrens *et al.* [15] to extract the proton axial vector form factor

$$G_A(Q^2) = \frac{g_A(0)(1 + \eta)}{2(1 + Q^2/M_A^2)}$$

where $g_A(0)$ and M_A are respectively the axial vector coupling constant and mass, and η is a parameter expected to be zero in the valence quark model plus $u\bar{u}$ and $d\bar{d}$ pairs in the quark sea. However, these measurements yielded a value of $\eta = 0.12 \pm 0.07$ which was interpreted to be due to either heavy quark currents (such as $s\bar{s}$) or a “nonstandard” axial-vector isoscalar current. If the former interpretation is adopted with the accepted value of $M_A = 1.032 \pm 0.036$ GeV, this leads to a value of $\Delta s = -0.15 \pm 0.09$ in remarkable agreement with the DIS analysis [16].

Finally, measurements of $p\bar{p}$ annihilation [17] at rest leading to $\phi\pi^+\pi^-$ and $\omega\pi^+\pi^-$ final states indicate that the ratio $\sigma(\phi\pi^+\pi^-)/\sigma(\omega\pi^+\pi^-) \sim 2 - 3\%$ in contrast to the expectation from the Okubo-Zweig-Iizuka (OZI) rule [18] of about 0.4%. Ellis *et al.* [19] have explained this in terms of “shake-out” and “rearrangement” diagrams by including $s\bar{s}$ pairs in the initial p and \bar{p} states, thus avoiding the discrimination against disconnected $q\bar{q}$ pairs in the OZI rule.

On the other hand, several papers have been published which explain many of these experimental observations without relying on any $s\bar{s}$ pairs in the quark sea. In particular, Lipkin has been able to account for the DIS results by assuming a *non* flavor symmetric sea containing $u\bar{u}$ and $d\bar{d}$ but no $s\bar{s}$ quark pairs [20].

Anselmino and Scadron [21] have used a modified $SU(6)$ valence quark model that allows for additional gluons and orbital angular momentum. When confronting the DIS results, they obtain a very small $\Delta s \approx -0.02$ at the ± 0.07 level. Stern and Clement [22] incorporate $SU(3)$ symmetry breaking to analyze the DIS results and find good agreement with experiment, while imposing $\Delta s = 0$.

Anselmino and Scadron have also applied their model to the discrepancy in the determination of the $\pi - N \sigma$ term. They obtain $\sigma_{\pi N} \approx 60$ MeV without resorting to additional strange quarks. McGovern and Birse have carried out an RPA calculation of the energy of the strange baryons and the $\sigma_{\pi N}$ term [23]. They obtain an expectation value of ≤ 0.05 for the $s\bar{s}$ content of the nucleon and a value of $\sigma_{\pi N} \approx 92$ MeV which, they acknowledge, is now too large, but they argue it can be improved by adding more mesons to the model.

While Close has argued that if strange quarks are assumed to be responsible for the νp form factor results discussed earlier, then agreement with DIS is obtained, he also addresses the other side of the story. If it is assumed instead that $\Delta s = 0$, then the data can be used to determine $M_A = 1.06 \pm 0.05$ GeV which is not in disagreement with the accepted value [16].

Lipkin (along with Zou) [24] has also demonstrated a possible breakdown of the OZI rule in the $p\bar{p}$ experiments. Thus it is not completely clear from the earlier measurements that there is convincing evidence for $s\bar{s}$ as constituents of the quark sea.

Given this situation, a direct measurement of the knockout of an $s\bar{s}$ pair from the nucleon ground state would therefore constitute incontrovertible proof of the existence of such pairs in the nucleon and would be sensitive to the probability of finding such a pair. Given that the ϕ meson is an almost pure $s\bar{s}$ pair, the observation of ϕ photoproduction would seem to satisfy this requirement. However, because the ϕ possesses the same quantum numbers as the photon, *i.e.* is a vector meson with $J^P = 1^-$, there is a large (dominant) amplitude for ϕ production through vector-meson-dominance (VMD) via which the photon (real or virtual) fluctuates into a vector meson such as the ϕ and interacts hadronically with the nucleon, scattering diffractively through Pomeron exchange. At small t this is expected to be the dominant amplitude for ϕ photoproduction. Thus the observation of direct $s\bar{s}$ knockout must be observed in interference with the VMD amplitude. This is the basis for the proposed experiment.

While we are proposing to look for $s\bar{s}$ pairs in the proton by measuring observables sensitive to a direct knockout process, there are other observables sensitive to the hidden strangeness. Parity-violating electron scattering can be used to probe the possible

strangeness content of the proton by measuring the strange form factors of the nucleon from the interference of the γ -exchange and the Z^0 -exchange amplitudes [25]. The SAMPLE [26] experiment ongoing at Bates is aimed at measuring the strange magnetic form factor of the proton at low Q^2 . The ongoing Jlab Hall A experiment HAPPEX is designed to look at the combination of the strange electric and magnetic form factors of the nucleon at low Q^2 . The Jlab G0 experiment will study both the strange magnetic and electric form factors systematically at low Q^2 region, and the Jlab Hall A parity violation experiment from ^4He by Beise *et al.* is aimed to investigate the strange electric form factor of the nucleon at low Q^2 . There are also a few relevant experiments at Jlab involving ϕ meson production which we will discuss in detail later. These efforts are complementary to the experiment proposed here.

II. THEORETICAL CONSIDERATIONS

The idea of looking for hidden strangeness in the nucleon, *i.e.* for $s\bar{s}$ pairs in the quark sea directly, originally proposed by Henley *et al.* [27], is to measure the amplitude for the direct knockout of such a pair in the form of a ϕ meson which is known to be nearly pure $s\bar{s}$. The difficulty with such a measurement is that other mechanisms contribute to ϕ production as well. Thus the problem (and the solution) is to attempt to find an experimental observable which is sensitive to the probability of finding the $s\bar{s}$ in the nucleon, rather than from some other mechanism(s). As we show later, the prediction based on the conventional mechanisms for dynamical production of the ϕ gives a negligible contribution to the polarization observables, while that due to pre-existing $s\bar{s}$ pairs contributes significantly.

The primary contribution to electromagnetic production of the ϕ is for the incoming photon (real or virtual) to fluctuate into a virtual vector meson (such as the ϕ) and then diffractively scatter from the nucleon by Pomeron exchange, thereby putting the vector meson on the mass shell, a mechanism known as vector meson dominance (VMD) [28] (see Fig. 1). Other contributions come from processes such as one pion exchange (OPE) (see Fig. 2) wherein either the photon fluctuates into the vector meson which then exchanges a pion with the nucleon target (Fig. 3(a)), or the photon fluctuates into a virtual ϕ - π state and the pion is absorbed by the target nucleon (Fig. 3(b)). Such processes have been interpreted as corrections to the primary VMD mechanism [29]. Other diagrams such as those with a ϕ - ϕ - π vertex are possible but are not found to be important in successful VMD calculations. [30] [31] These calculations have fit data well. Other diagrams, such as ρ or ω exchange are forbidden by C-parity conservation. Hence, there is no vector meson exchange.

The success of VMD model has been investigated in recent years within the framework of QCD. It was shown [32] that the interpretation of Pomeron-exchange in terms of gluon-exchange is consistent with the quark-substructure of vector mesons. At the low Q^2 considered in this proposal, the usual VMD parameterization of diffractive amplitude is valid.

As is usual when searching for weak reaction amplitudes in the presence of a stronger one the knockout amplitude is determined by measuring its interference with the larger VMD amplitude. Polarization observables are one of the standard tools for measuring such interferences.

The cross sections and polarization observables for ϕ photo- and electroproduction have recently been calculated by Titov *et al.* [33]. The results of these calculations are (1) both the VMD and $s\bar{s}$ knockout contributions are strongly forward peaked, *i.e.* are largest at small momentum transfer, t ; (2) with an assumed 1-2% admixture of $s\bar{s}$ quarks in the nucleon, the knockout cross section is $\sim 10\%$ of that for VMD; (3) the OPE contribution to the cross section is approximately equal to that for $s\bar{s}$ knockout; and (4) the uud knockout process, in which the $s\bar{s}$ quarks are spectators, becomes large, and perhaps dominant, at large momentum transfer (very backward angles for the ϕ). However, with regard to this last point, the cross section is still smaller than that at forward angles by about two orders of magnitude. The diagrams for $s\bar{s}$ and uud knockouts are shown in Fig. 4.

Before discussing the calculated polarization observables in detail, we present here a few general considerations regarding them. First of all, the single photon polarization asymmetries are not sensitive to the strangeness content of the nucleon [33]. For real photons, the single transverse photon polarization must vanish in the limit as the reaction angle goes to zero. For large angles the cross section rapidly decreases. Single longitudinal polarization observables are zero from parity conservation. Thus, the conclusion is that double polarization observables offer the highest sensitivity to the knockout process.

The possible double polarization asymmetries observable with polarized photons are beam/vector meson (or γ^*/ϕ where γ^* is a real or virtual photon) where the cross section is determined for polarized incident photons and measured vector meson polarizations, beam/target (or γ^*/p) in which the beam and target polarizations are controlled, and beam/recoil (or γ^*/p') in which the photon polarization is controlled and the recoil proton polarization is measured.

Since in the diffractive VMD process, the outgoing vector meson ϕ must have the same polarization as the incoming photon, there will be a large asymmetry in the beam/vector meson double polarization just due to this process, *i.e.* the cross section will be large for parallel polarizations and small for the antiparallel case. Any effects due to small reaction amplitudes will be dwarfed. For polarized photons, this leaves the beam/target or beam/recoil double polarization asymmetries. Since the VMD process does not flip the target spin and thus the recoil proton will have the same spin as the target, the pure VMD contribution to either of these asymmetries is expected to be small. Thus these two asymmetries are the most likely to have sensitivity to the knockout amplitude.

In the diffractive VMD process, as we have mentioned, the vector meson ϕ has the same spin polarization as the incoming photon. For a polarized target this means we expect very little beam-target asymmetry due to the VMD mechanism alone. On the other hand, for the knockout mechanism, reversing the target polarization is equivalent to reversing the spectator uud polarization in the $|uud\rangle \otimes |s\bar{s}\rangle$ target. The $s\bar{s}$ in the target proton can couple to either $J^P = 1^-$ or 0^- . This pair then couples to the uud $J^P = 1/2^+$ core configuration in a state of orbital angular momentum $L = 1$ so that the spin and parity of the $|uud\rangle \otimes |s\bar{s}\rangle$ total wave function is $1/2^+$. The largest contribution to the electromagnetic excitation of the target $s\bar{s}$ pair to a ϕ ($J^P = 1^-$) arises from the $0^- \rightarrow 1^-$ transition. Hence the proton configuration with the largest contribution to the knockout mechanism is a 0^- $s\bar{s}$ pair coupled to the $1/2^+$ uud valence quark configuration in a relative $L = 1$ state (P -wave). Thus, the projection of the orbital angular momentum along the proton spin axis must be $M = 0$. Reversing the orientation of the target spin reverses the orientation of the uud

valence quark configuration in the target proton and flips the sign of the coupling coefficient from $\sqrt{1/3}$ to $-\sqrt{1/3}$ and, hence, also the sign of the knockout amplitude relative to the sign of the VMD amplitude. Thus we expect to observe a large asymmetry in the beam/target asymmetry. Similar arguments also apply to the beam/recoil asymmetry.

Titov *et al.* have calculated the various double polarization asymmetries: beam/target, beam/recoil, and beam/vector meson. Their results confirm the naive arguments given here. First of all, the beam/vector meson polarization asymmetry is almost entirely due to the VMD mechanism with extremely little sensitivity to the knockout mechanism. Both the beam/target and beam/recoil polarization asymmetries exhibit large effects due to including $s\bar{s}$ quarks in the proton provided the incoming photon is circularly polarized with the helicity along its momentum direction. For the beam/recoil asymmetry, the largest sensitivity to the percentage of strange quarks in the target occurs for a recoil polarization P'_x (transverse to the proton momentum direction and in the reaction plane) for ϕ CM angles of $45^\circ - 60^\circ$. P'_z polarization observables (along the recoil proton momentum direction) are largest for ϕ CM angles near 180° , indicating they are primarily due to the uud knockout with an $s\bar{s}$ spectator. However, we repeat that the cross sections are small at backward angles.

Specifically, Fig. 5 shows the photoproduction beam/recoil double polarization asymmetry L_{zx}^{BR} for the four possible combinations of the phases of the $s\bar{s}$ configurations with $J^P = 0^-$ and 1^- . These calculations [33] were done using a relativistic harmonic oscillator model [34], an improvement over the original model used by Henley *et al.* [27] which used a nonrelativistic constituent quark model. The VMD amplitude was calculated using the model proposed by Donnachie and Landshoff [30] and developed by others [31] where the Pomeron is described in terms of a non-perturbative multi-gluon exchange. The VMD contribution to the asymmetries shown in Fig. 5 includes the OPE corrections. These calculations also include contributions from both 0^- and 1^- $s\bar{s}$ pairs (in contrast to the naive arguments given earlier), *i.e.* the wave function of the proton in Fock space is given by [27] [33]:

$$|p\rangle = A|[uud]^{1/2}\rangle + B\{a_0|[uud]^{1/2} \otimes [s\bar{s}]^0]^{1/2} + a_1|[uud]^{1/2} \otimes [s\bar{s}]^1]^{1/2}\}$$

with B^2 the probability of finding $s\bar{s}$ pairs in the proton and a_0 and a_1 the relative amplitudes for those pairs being in 0^- and 1^- configurations. It is the unknown phase between amplitudes a_0 and a_1 which accounts for the four panels in Fig. 5.

Two separate amplitudes are calculated for the knockout process depending on which quark is struck by the photon: (1) $s\bar{s}$ knockout with a uud spectator, and (2) uud knockout with an $s\bar{s}$ spectator. Both are included in the asymmetry. Clearly the latter is dominated by the component of the proton wave function with $s\bar{s}$ coupled to 1^- given by amplitude a_1 . The calculations further confirm that the first process, the direct $s\bar{s}$ knockout with a uud spectator, is dominated by the target wave function with $s\bar{s}$ pairs coupled to 0^- , associated with the amplitude a_0 .

Finally, the calculations show that the optimal range of initial photon energy is 2-3 GeV. The contribution of the knockout mechanism at higher photon energy is suppressed due to a rapid decrease in the form factors.

Both these calculations [33] and those of Henley [27] were done for real photons. We have used these to show the general sensitivity to the strangeness content. However, Titov

[35] has recently expanded his calculations to investigate the polarization asymmetries in electron scattering. Thus, we propose to probe the same physics using virtual photons. We proceed with some general considerations relating electron scattering to the results of the discussion so far, with the explicit aim of choosing the best kinematics.

The proposal being presented here utilizes the high resolution offered by the Hall A HRS system to reconstruct the ϕ mass with sufficient accuracy to obviate the need for direct detection of the $\phi \rightarrow K^+K^-$ in the final state. As such, the electron arm HRS (HRSe) is effectively being used to tag the virtual photon. The virtual photon is polarized by polarizing the incident electron.

In the context of the presently proposed experiment, it is useful to cast the differential cross section following the formalism of Donnelly and Raskin [36] into the following form,

$$\frac{d^5\sigma}{dE'd\Omega_e d\Omega_p^c} = \frac{d^2\sigma}{d\Omega_p^c} \Gamma \quad (1)$$

where the virtual photoproduction cross section in the photon/target CM frame is

$$\frac{d^2\sigma}{d\Omega_p^c} = \sigma_{\gamma^*} \{2\rho_L \epsilon R_L + R_T - \sqrt{\rho_L \epsilon (1 + \epsilon)} R_{TL} - \epsilon R_{TT} + h(-\sqrt{\rho_L \epsilon (1 - \epsilon)} R_{TL'} + \sqrt{1 - \epsilon^2} R_{T'})\} \quad (2)$$

with the point photoproduction cross section given by

$$\sigma_{\gamma^*} = \frac{\alpha}{4\pi} \frac{M_\phi M_p^2 P_\phi^c}{W(W^2 - M_p^2)} \quad (3)$$

and where

$$\Gamma = \frac{\alpha}{2\pi^2} \frac{E'}{E} \frac{W^2 - M_p^2}{2M_p(-Q^2)} \frac{1}{1 - \epsilon} \quad (4)$$

is the virtual photon flux [36]. The longitudinal polarization ϵ is given by $\{1 - 2(q^2/Q^2)\tan^2(\vartheta_e/2)\}^{-1}$, and $\rho_L = (-Q^2/q^2)(W/M_p)^2$ with Q^2 (less than zero) being the square of the transferred four-momentum and q^2 for the three-momentum, now all evaluated in the lab frame. Hadron angles and momenta are evaluated in the CM frame.

In the absence of measuring recoil or target polarization, the fifth response function has an explicit out-of-plane dependence given by $\sin\varphi_p^c$ and, thus, vanishes for in-plane measurements. However, that is not true in the case where the recoil polarization is measured. It becomes a sum of terms either $\sin\varphi_p^c$ or $\cos\varphi_p^c$ depending on which polarization orientation of the outgoing proton is being measured. Unfortunately, in the case of measuring P'_x , it goes as $\cos\varphi_p^c$, and thus is largest in-plane. The virtual photon polarization associated with the sixth response function $R_{T'}$ is purely circular. The surviving in-plane parts of $R_{TL'}$ will dilute this polarization (although they may provide useful information). Thus the circular polarization of the virtual photon about the \hat{q} -direction is maximized by minimizing the ratio of the kinematic factors $|v_{TL'}/v_{T'}| = \sqrt{\rho_L \epsilon / (1 + \epsilon)}$, while maintaining $v_{T'}$ itself to be as large as possible.

This tends to drive Q^2/q^2 towards zero, *i.e.* toward the real photon limit, and moreover to have ϵ as small as possible. This also leads to a small scattered electron energy such that one is operating near the “end point” of the virtual photon spectrum. This introduces two complications, first with operating the HRSe at too low a momentum and, second, a large background in the spectrum due to a growing radiative tail from elastic $e\bar{p}$ scattering at very large ω/E_0 where E_0 is the incident electron energy and ω is the electron energy transfer.

Thus, the chosen kinematics represent a compromise to maximize the transferred polarization while minimizing background contributions and maintaining the HRSe in a comfortable operating regime.

The results of the electron scattering calculations [35] explicitly performed for these kinematics are displayed in Figs. 6-7 and confirm the qualitative arguments just given. In comparison with the real photon result of Fig. 5, the asymmetry is slightly less, due to the dilution of the photon polarization, but this is more than offset by the large improvement in luminosity afforded by the electron beam.

Clearly, the theoretical predictions presented in Figs. 5-7 depend strongly on the accuracy of the employed VMD model in describing the diffractive amplitude. This question has been addressed partially in Ref. [32]. It can be shown [37] that the VMD parameterization employed by Titov *et al.* is consistent with the quark-substructure of the ϕ meson in the low Q^2 region considered in this proposal. A refined VMD model including the spin-dependence in Pomeron-exchange is being developed for improving the theoretical predictions directly related to the experiment being proposed here.

III. PROPOSED MEASUREMENTS

We propose to perform the measurement of $p(\bar{e},e'\bar{p})\phi$ in Hall A at Jlab with longitudinally polarized electrons and the focal plane polarimeter (FPP) at $|Q^2| = 0.135 \text{ (GeV/c)}^2$ with an incident electron beam energy of 3.0 GeV. The scattered electrons and protons will be detected in coincidence and the reconstructed missing mass technique will be used to identify the undetected ϕ mesons. The invariant mass of the virtual photon and proton system is fixed at a central value of 2.15 GeV, and the hadron arm HRS is set corresponding to the ϕ meson angle of 48° in the center-of-mass frame of the virtual photon and the proton.

The calculation [33] of the photoproduction of a ϕ meson from a proton target shows that the beam-recoil asymmetry $L_{zx'}^{BR}$ is just as sensitive to the $\bar{s}s$ content of the proton as that of the longitudinal beam-target asymmetry $L_{zz'}^{BT}$, where z is along the photon momentum direction, and x' is in the reaction plane and transverse to the recoil proton momentum direction in the final ϕ -proton center-of-mass system. Fig. 5 shows the calculated beam-recoil asymmetry $L_{zx'}^{BR}$ as a function ϕ angle in the center-of-mass frame of the real photon and the proton system at an invariant mass of 2.15 GeV. The solid line is for VMD+OPE (no strangeness in proton), the dash-dotted line and the dashed line correspond to an $\bar{s}s$ admixture of 0.25% and 1% in the proton, respectively. The four panels correspond to four possible phase combinations for the two spin configurations of $\bar{s}s$ in the proton as described in Section II.

Based on this theoretical prediction and due to the experimental complications and the low luminosity associated with the tagged photon flux and the solid polarized proton target,

we propose this measurement with a longitudinally polarized electron beam and a focal plane polarimeter to measure the recoil proton polarization from $p(\vec{e}, e'\vec{p})\phi$. Recently, the double polarization observables from $\gamma^*p \rightarrow p\phi$ were calculated for the first time by Titov *et al* [35] at the proposed kinematic setting of this experiment. The sensitivity to $\bar{s}s$ content of the proton is slightly reduced compared with the real photon case which is expected from our simple argument of different response functions of electron scattering in Section II. At the 3.0 GeV kinematic setting, the beam-recoil asymmetry is still very sensitive to the strangeness content of the proton as we anticipated. Fig. 6 shows the calculated beam-recoil asymmetry $L_{zz'}^{BR}$ from electroproduction of ϕ mesons from protons at the following kinematic setting: $E_0 = 3.0$ ($|Q^2| = 0.135$ (GeV/c) 2). Fig. 7 shows the calculated $L_{zz'}^{BR}$ at the above kinematic setting. Figs. 8-9 show the proposed measurements of the recoil proton polarization component $P_{x'}$ and $P_{z'}$, which are defined as $L_{zx'}^{BR}$ and $L_{zz'}^{BR}$ in Ref. [33] with the electron helicity being along its momentum direction.

There are two approved experiments and one conditionally approved experiment at Jlab on ϕ meson production. All three experiments will be carried out in Hall B. Experiment E93-031 [38] will study the photoproduction of vector mesons at high t to study hidden-color components in hadronic matter. The kinematic region focussed in E93-031 is very different from this proposal as our kinematics is in the small t region. Furthermore, this experiment is a double polarization experiment which is expected to be very sensitive to the direct knock-out of strange quark anti-quark pairs from the proton.

Approved experiment E93-022 [39] will measure the polarization of the ϕ meson in electroproduction from a proton target by measuring the angular distribution of the decay kaons. This is a single polarization measurement which aims to measure the fraction of ϕ production due to the pseudoscalar exchange mechanism relative to diffractive scattering with a sensitivity at the level of $\sim 5 - 10\%$. Although ϕ production from a proton target through direct knockout of an $\bar{s}s$ is expected to exchange a pseudoscalar meson dominantly, π -exchange and η -exchange diagrams contribute to ϕ production because of the decay properties of ϕ mesons. Thus, the sensitivity to the $\bar{s}s$ content in the proton is limited by measuring this single polarization observable.

Conditionally approved experiment PR97-005 [40] proposes to measure photoproduction of ϕ meson with linearly polarized photons. The spin density matrix elements will be extracted by measuring the decay kaon angular distribution. The measurement is expected to be sensitive to new reaction mechanisms other than diffractive scattering or pseudoscalar meson exchange. Because of the dominance of VMD diffractive scattering at forward angles in ϕ photoproduction and electroproduction, the beam-vector meson double polarization observable is not sensitive to the direct knockout of $\bar{s}s$ component of the proton. Thus, our experiment is more sensitive to the strange quark content of the proton, and it is complementary to the Hall B ϕ experiments discussed above.

We emphasize that this experiment will utilize fully the unique features of Hall A: the high luminosity and high resolution spectrometers. This experiment will provide in a timely way the very important measurement probing the strangeness content of the proton using electroproduction of the ϕ meson with double polarizations. This initial measurement will motivate more theoretical work in this direction which certainly will help to interpret the data in a less model-dependent way. Furthermore, this measurement will be complementary to any future Hall B experiments in which a polarized tagged photon beam and a polarized

solid proton target will be employed, thus providing cross check of the theory. This experiment will also motivate future experiments in Hall A with polarized electron beam and the FPP on the ϕ meson production at higher energies (8-12 GeV).

IV. THE EXPERIMENT

A. Experimental Overview

This experiment requires a longitudinally polarized electron beam with polarization 80% at a beam current of $50\mu\text{A}$. The experiment will employ the Hall A cryogenic liquid hydrogen target, both the electron and the hadron high resolution spectrometers (HRS), and the FPP. One electron beam energy: 3.0 GeV is required. We will use the missing mass technique to identify the undetected ϕ meson by measuring the scattered electrons and protons in coincidence $p(\vec{e}, e'\vec{p})\phi$. Fig. 10 shows the previous measurement of $p(e, e'p)X$ [41] as a function of the missing mass squared. Even with a missing mass squared resolution of $\sim 0.1 \text{ GeV}^2$, one can see the ϕ mass peak. With the Hall A high resolution spectrometers, the missing mass squared resolution will be improved by about a factor of 10, limited by the intrinsic width of the ϕ and multiple scattering in the LH2 target, thus improving the signal-to-background ratio by a factor of 10 for the $p(e, e'p)\phi$ measurement. Table I lists the kinematic setting for this experiment.

B. The Polarized Electron Beam

Given the technical developments achieved over the years with strained GaAs cathodes at SLAC, Mainz and NIKHEF and bench tests at Jlab, high electron polarization (80%) is possible to achieve at TJNAF. The first Jlab experiment [42] which requires high electron polarization at a beam current of $15\mu\text{A}$ is scheduled to run in the fall of 1998. The recently achieved performance of the Mainz polarized electron source is very encouraging in terms of high electron polarization at very large beam current. The polarization of the beam will be measured with the Hall A Möller and/or Compton polarimeter. We note that we request a beam current of $50\mu\text{A}$ at an electron polarization of 80% in this proposal.

C. The Focal Plane Polarimeter

The Hall A focal plane polarimeter consists of a graphite analyzer with two straw chambers upstream and two downstream for tracking of protons. The analyzer consists of 5 sets of graphite plates with thicknesses of 3.2, 6.4, 12.9, 25.9, and 38.9 g/cm^2 (0.75, 1.5, 3.0, 6.0, and 9.0 inches), which can be used in any combination. The analyzer covers the full spectrometer acceptance. Each chamber consists of six planes of straws (3 U and 3 V for all chambers except for the one immediately after the analyzer, which has 2 U, 2 V, and 2 X). This gives sufficient redundancy that tracking efficiency is close to 100% over the entire active area. Angular resolution of tracks is about 4 mr. For the kinematics of this experiment, the average analyzing power is 0.5 (0.683 GeV/c protons). The efficiency for events

scattered between 5° and 20° is about 4%, as determined in experiments at LAMPF, Mainz, PSI and TRIUMF.

D. Simulations

For the two-body process $\gamma^*p \rightarrow \phi p$ of interest, one can reconstruct the three momentum and the energy of the undetected ϕ meson, hence its mass by accurately determining the recoil proton momentum and angle. Thus, it is very important to have fine resolution in the reconstructed ϕ mass to reject backgrounds. Since the proposed experiment relies on the missing mass technique to identify the undetected ϕ meson events, it is very important to simulate the missing mass resolution for ϕ meson reconstruction at the kinematics of this experiment. A Monte Carlo simulation code was written for this purpose.

In our simulation, we used $\sigma(E)/E = 1.0 \times 10^{-4}$ for the beam energy resolution and $\delta p/p = 1 \times 10^{-4}$ (RMS) for the momentum resolutions of both spectrometers. For the spectrometer angular resolutions (RMS), 0.6 mr and 2.0 mr were used for the horizontal and vertical, respectively. Multiple scattering in the target, windows, and air gaps were included in the simulation, as well as straggling and energy loss for the outgoing particles. For the kinematics of our proposed measurements, the missing mass resolution is dominated by multiple scattering in the target in the hadron arm. The missing mass squared resolution (FWHM) from kinematic reconstruction only is around 0.01 GeV^2 . The total missing mass squared resolution is $\sim 0.013 \text{ GeV}^2$ which includes the natural decay width of the ϕ meson. Thus, the missing mass squared resolution of this experiment will be improved by a factor of 10 than that was achieved in the earlier measurement. Fig. 11 shows the simulated missing mass squared resolution at the kinematics of this experiment. $\langle \theta_e \rangle = 12.6^\circ$, and $887.19 \leq E' \leq 980.57 \text{ MeV}$. This corresponds to $|\langle Q^2 \rangle| = 0.135 (\text{GeV}/c)^2$ and $\langle W \rangle = 2.15 \text{ GeV}$. The central momentum and angle settings for the hadron arm are $683.0 \text{ MeV}/c$ and 34.47° in the simulation. With this kind of missing mass squared resolution, a missing mass squared cut of $m_\phi^2 - 0.01 \leq M_{\text{missing}}^2 \leq m_\phi^2 + 0.01 (\text{GeV}^2)$ can reject the backgrounds efficiently as will be discussed later in this proposal.

E. Backgrounds

For the proposed $p(\vec{e}, e'\vec{p})\phi$ measurement, one can effectively rewrite the reaction in terms of the following two-body process: $\gamma^*p \rightarrow p\phi$. Thus, dominant two-body final state background channels will be rejected by the missing mass cut on the ϕ mass peak. The remaining backgrounds come mostly from three contributions which we will discuss in detail below.

The accidental coincidence background is estimated in the following way. We used the Lightbody and O'Connell codes to calculate the singles electron and proton rates at all three kinematic settings of this experiment. To calculate the accidental coincidence rate, a coincidence timing cut of 3 ns was used. One can further reduce the coincidence rate by requiring a vertex cut. At the kinematics of this experiment, a factor of 10 reduction in the accidental coincidence rate can be achieved easily by applying a vertex cut, based on the quoted HRS transverse vertex resolution of 1.5 mm at 90° . The accidental coincidence

background as a function of missing mass was simulated at the kinematic setting of this experiment and its contribution to the ϕ signal is small as shown in Fig. 12. A modest factor of 5 reduction in the accidental coincidence rate using the vertex cut was applied in the simulation.

The primary sources of physics backgrounds to this measurement are the the multi-pion background, which is dominated by the $\pi^+\pi^-$ channel, and the s-wave K^+K^- productions [44]. An estimate of $1.5 \mu\text{b}$ for the total resonant plus nonresonant s-wave K^+K^- photoproduction cross section, together with the knowledge of the differential cross section for the ϕ meson photoproduction at a photon energy of around 2.1 GeV, allows us to estimate the cross section for $\gamma^*p \rightarrow pK^+K^-$ at the kinematics of this experiment. The s-wave K^+K^- production was simulated for this experiment as a function of missing mass squared. Fig. 12 shows the contribution of K^+K^- as slanted hatches. The $\pi^+\pi^-$ background was simulated in the same way as that of the K^+K^- channel, with the total electroproduction cross section measured from DESY [45] in the similar kinematic region as in this experiment. The simulated $\pi^+\pi^-$ contribution is shown as horizontal hatches in Fig. 12. The overall signal-to-background ratio is about 2:1 with a missing mass squared cut of $\pm 0.01 \text{ GeV}^2$ with respect to the ϕ mass peak. This estimate is consistent with the previously cited work on $p(e,e'p)X$ by Ahrens *et al.* [15] at similar t and W kinematic setting. As a cross check of our understanding of the overall background, thus the overall signal-to-background ratio for this experiment, we reproduced the observed signal-to-background ratio in Fig. 10 using the quoted resolution of that experiment and Henley's diffractive calculation of the ϕ signal.

F. Counting Rates

To estimate the coincidence rate for $p(e,e'p)\phi$ measurement, we followed the cross section formula derived by Henley *et al.* [27] from the vector meson dominance model of diffractive production of the vector meson, which was cross checked by the cross section calculation from Ref. [35]. The five-fold differential cross section is formed by $\frac{d^5\sigma}{dE'd\Omega_e d\Omega_p}$ for the coincidence measurement. Table II lists the calculated differential cross section, singles and the coincidence rates at the proposed kinematics with the spectrometer acceptances taken into account. In estimating the rates, we assumed a beam current of $50 \mu\text{A}$. This corresponds to a luminosity of $2.0 \times 10^{38}/\text{cm}^2$ for a 15-cm LH2 target cell. For each spectrometer, we used 5.5 msr solid angle for extended target and 0.9 for detection efficiency. In addition, we used a scattered electron energy bin of 80 MeV.

Given the p , π^+ , e , and π^- rates from Table II, the expected overall trigger rate would be 7600 Hz in a 100 ns window, totally driven by accidental coincidences. This is too high for the Hall A DAQ system (2 kHz limit). Therefore, we propose to run with both the electron and hadron arm Čerenkov detectors in veto mode. This reduces the accidental rate and, hence, the trigger rate to a modest 684 Hz. There may be a few percent loss of good events due to the Čerenkov rate, but the asymmetry will be unaffected.

G. Beam Time Estimate

The beam-recoil asymmetry $L_{zx'}^{BR}$ defined in Ref. [33] corresponds to the recoil proton polarization component $P_{x'}$ with the incident electron beam longitudinally polarized along its momentum direction, z is along the virtual photon three-momentum direction and x' is transverse to the recoil proton momentum direction z' , in the center of mass system of the incident photon and the target proton in the scattering plane.

By Fourier analysis of the azimuthal distribution of FPP events, two independent components can be extracted each with a statistical accuracy of

$$\delta P = \frac{\pi}{2\bar{A}_y} \sqrt{\frac{1}{fN}}, \quad (5)$$

where \bar{A}_y is the mean analyzing power, and f is the FPP efficiency, which is defined as the ratio of the events that are accepted by FPP for polarization analysis to the total number, N , of the spectrometer events. For coplanar kinematics the recoil proton polarization vector, \vec{P} , can be expressed as

$$\vec{P} = P_{yy}\hat{y}y + h(P_{xx'}\hat{x}x' + P_{zz'}\hat{z}z') \quad (6)$$

where $\hat{z}z'$ is along the nucleon momentum direction, $\hat{x}x'$ is in the reaction plane and transverse to the momentum, and $\hat{y}y'$ is normal to the reaction plane in the laboratory frame. The polarization measured in the focal plane \vec{P}^{fp} , is then

$$P_{xx'} = P_2^{fp} \quad (7)$$

$$P_{yy} = P_1^{fp}\cos\chi - P_3^{fp}\sin\chi \quad (8)$$

$$P_{zz'} = P_1^{fp}\sin\chi + P_3^{fp}\cos\chi \quad (9)$$

where P_1^{fp} is in the dispersion direction, P_2^{fp} is normal to the bend plane, P_3^{fp} is along the trajectory and χ is the spin precession angle.

In order to extract the polarization component of interest $P_{x'}$, which is expected to be sensitive to the strange quark content of the proton and which is calculated in the center-of-mass frame of the incident photon and the target proton, we need to measure both the $P_{xx'}$ and the $P_{zz'}$ components in the laboratory frame. Although P_3^{fp} can not be measured with the FPP, the fact that $P_{zz'}$ changes sign with the beam helicity whereas P_{yy} does not allows separation of the focal-plane polarization within the spectrometer bend plane into two independent reaction components P_{yy} and $P_{zz'}$. Thus, all three components of the recoil proton polarization can be determined from the FPP for this experiment.

By flipping the beam helicities, all three polarization components can be measured with the following statistical uncertainties:

$$\delta P_{xx'} = \frac{\delta P}{h} \quad (10)$$

$$\delta P_{yy} = \frac{\delta P}{\cos(\chi)} \quad (11)$$

$$\delta P_{zz'} = \frac{\delta P}{h\sin(\chi)} \quad (12)$$

The spin precession angle for the kinematics of this experiment is around 100° . Note that the beam-recoil asymmetry $L_{zz'}^{BR}$ is calculated in the center-of-mass frame of the incident photon and the target proton, thus transformations were performed to calculate the statistical uncertainty in $P_{x'}$ measurement for given beam time from the FPP measurements. In calculating the statistical uncertainty, an electron beam polarization of 80% was assumed. At the kinematics of this proposal, the FPP efficiency is about 4% and the average analyzing power is $\sim 50\%$, which are consistent with results obtained from FPP commissioning. The statistical uncertainties of $P_{x'}, P_{z'}, P_{y'}$ in 300 hours of running time are listed in Table II. For the production running of the experiment, we request a total of 300 hours of beam time. In addition, we request 24 hours for spectrometer and detector checkout and 24 hours for empty target measurement. In total, we request 348 hours of beam time (15 days) for this experiment.

H. Systematic Uncertainties

The systematic uncertainty of the beam-recoil asymmetry $L_{zz'}^{BR}$ ($P_{x'}$) measurement is dominated by the systematic uncertainties in the electron beam polarization measurement and the FPP measurement. The electron beam polarization will be determined by the Hall A Möller polarimeter/Compton polarimeter and a 4% overall uncertainty can be achieved for the polarization measurement.

The major systematic uncertainties related to the FPP are the knowledge of the analyzing power and instrumental asymmetries. The analyzing power of graphite for protons in the energy range of interest in this experiment has been measured at LAMPF, PSI, and TRI-UMF. The overall uncertainty for the world average is estimated to be $\pm 2\%$ [46]. Based on the analysis of Jlab experiment 89-033, instrumental asymmetries (ϵ_{inst}) are expected to be about 0.005, corresponding to an uncertainty in the measured polarization of about ϵ_{inst}/A_c , about 0.012. However, by combining opposite helicity states, the instrumental asymmetry contribution to the measurement of P_x and P_z cancels to first order. Both the uncertainty on the analyzing power and the instrumental asymmetries are thus both expected to contribute less to the absolute uncertainty than the measurement of beam polarization, and be less than the statistical uncertainty.

The asymmetry from background contribution can be determined and corrected from the data to obtain the ϕ asymmetry by measuring the recoil proton polarization on both sides of the ϕ mass peak. This procedure is justified by the missing mass technique proposed in this experiment because the ϕ production channel and all other background channels are showed up in the missing mass spectrum as an incoherent sum. Thus, one does not have to worry about the interference effects among different reaction channels. This is opposite to the case in which one of the kaons is tagged in the measurement. The systematic uncertainty in the polarization correction due to backgrounds is estimated to be smaller than the statistical uncertainty of the measurement. The beam-recoil asymmetry from background channels of K^+K^- and $\pi^+\pi^-$ are currently being calculated by our theory collaborators.

V. COLLABORATION BACKGROUND AND RESPONSIBILITIES

This experiment requires the longitudinally polarized electron beam, the standard Hall A liquid hydrogen target, and both Hall A HRS spectrometers. The recoil proton polarization will be measured using the focal plane polarimeter. This experiment will run with standard Hall A equipment. Many members in our collaboration have extensive experience in polarization experiments with longitudinally polarized electron beams. at Jlab and many other laboratories. The Rutgers group along with William and Mary and other institutions are responsible for the construction and commissioning of the Hall A FPP. Many members of this collaboration have significant experience in running experiments in Hall A. Members of the MIT group together with Hall A staff and others led the first Hall A collaboration experiment. Currently, the MIT group is actively engaged in the polarized ^3He program in Hall A. The University of New Hampshire group is responsible for the Hall A trigger system and is planning on upgrade of the Hall A scintillators to improve timing resolution by a factor of two. They are also experienced in Hall A running. The expertise and manpower of this collaboration is adequate to carry out this program. This collaboration also has very strong theoretical support.

VI. ACKNOWLEDGEMENTS

We acknowledge helpful discussions with R.D. McKeown, E. Smith and R. Williams.

TABLES

E (GeV)	E' (GeV)	θ_e (degree)	P_p (GeV/c)	θ_q (degree)	θ_p (degree)	W (GeV)	$ Q^2 $ (GeV/2) ²	ϵ
3.0	0.934	12.6	0.683	-5.57	-34.47	2.15	0.135	0.557

TABLE I. Kinematics for the proposed $p(\vec{e}, e'\vec{p})\phi$ reaction. The negative sign indicates that the hadron arm is on the opposite side of the beam line compared with the scattered electron direction. W is the invariant mass for the virtual photon and proton system and ϵ is the polarization of the virtual photon.

E (GeV)	$d^5\sigma/(dE'd\Omega_e\Omega_p)$ (nb/GeVsr ²)	$p(e, e'p)\phi$ (Hz)	Beam time (hours)	$\Delta p_{x'}$	$\Delta p_{z'}$	$\Delta p_{y'}$	(e, e') (Khz)	(e, p) (Khz)	(e, π^+) (Khz)	(e, π^-) (Khz)
3.0	2.9	1.2	300.0	0.029	0.028	0.11	60.0	114.3	190.0	190.0

TABLE II. Rate estimate and beam time request for the proposed $p(\vec{e}, e'\vec{p})\phi$ measurement.

REFERENCES

- [1] see *e.g.* Nathan Isgur in “Modern Topics in Electron Scattering”, B. Frois and I. Sick (eds.), World Scientific, 1991, pp. 2-27, and the references therein.
- [2] G. Höhler, in Landolt-Börnstein. vol. 9b2, ed. H. Schopper (Springer-Berlin, 1988).
- [3] R. Koch, Z. Phys. **C15**, 161 (1982).
- [4] T. P. Cheng and R. F. Dashen, Phys. Rev. Lett. **26**, 594 (1971); T. P. Cheng, Phys. Rev. **D13**, 2161 (1976).
- [5] J. Gasser, H. Leutwyler, and M. E. Sainio, Phys. Lett. **B253**, 252 (1991).
- [6] M. J. Alguard *et al.*, Phys. Rev. Lett. **37**, 1261 (1976); M. J. Alguard *et al.*, Phys. Rev. Lett. **41**, 70 (1978); V. W. Hughes *et al.*, Proc. Lausanne Symp. 1980, p. 331 (SLAC-PUB-2674, 1981).
- [7] EMC (J. Ashman *et al.*), Phys. Lett. **B206**, 364 (1988); EMC (J. Ashman *et al.*), Nucl. Phys. **B328**, 1 (1989).
- [8] J. Ellis and R. Jaffe, Phys. Rev. **D9**, 1444 (1974).
- [9] SMC (D. Adams *et al.*), Phys. Lett. **B329**, 399 (1994); SMC (A. Witzmann *et al.*), Nucl. Phys. **A577**, 319c (1994); SMC (D. Adams *et al.*), Phys. Rev. **D56**, 5330 (1997); SMC (B. Adeva *et al.*), Phys. Lett. **B412**, 414 (1997).
- [10] E142 (P. L. Anthony *et al.*), Phys. Rev. Lett. **71**, 959 (1993).
- [11] E143 (K. Abe *et al.*), Phys. Lett. **B364**, 61 (1995). E143 (K. Abe *et al.*), Phys. Rev. Lett. **74** 346 (1995)
- [12] E154 (K. Abe *et al.*), Phys. Rev. Lett. **79**, 26 (1997).
- [13] HERMES (K. Ackerstaff *et al.*), Phys. Lett. **B404**, 383 (1997).
- [14] J. Ellis and M. Karliner, Phys. Lett. **B341**, 397 (1995); see also the plot on the SLAC E155 web site.
- [15] L. A. Ahrens *et al.*), Phys. Rev. **D35**, 785 (1987).
- [16] F. E. Close, Phys. Rev. Lett. **64**, 361 (1990).
- [17] J. Reifenröther *et al.*), Phys. Lett. **B267**, 299 (1991); C. Amsler *et al.*), Phys. Lett. **B346**, 363 (1995); A. Bertin *et al.*), Phys. Lett. **B388**, 388 (1996).
- [18] G. Zweig, CERN Report 8419/TH412, 1964 (unpublished); S. Okubo, Phys. Lett. **5**, 165 (1963); I. Iizuka, K. Okada, and O. Shito, Prog. Theor. Phys. **35**, 1061 (1966).
- [19] J. Ellis and M. Karliner, Invited lectures at the International School of Nucleon Spin Structure, Erice, 1995, CERN Report No. CERN-TH/95-334 (1995); hep-ph/9601280, and references therein.
- [20] Harry J. Lipkin, Phys. Lett. **B256**, 284 (1991).
- [21] M. Anselmino and M.D. Scadron, Phys. Lett. **B229**, 117 (1989).
- [22] Jacqueline Stern and Gerard Clement, Phys. Lett. **B231**, 471 (1989).
- [23] J. A. McGovern and M. C. Birse, Phys. Lett. **B209**, 163 (1988).
- [24] H. J. Lipkin and B.S. Zou, Phys. Rev. **D53**, 6693 (1996).
- [25] R.D. Mckeown, Phys. Lett. **B 219** (1989) 140; D. Beck, Phys. Rev. **D 39** (1989) 3248.
- [26] B. Mueller *et al.*, Phys. Rev. Lett. **78**, 3824 (1998).
- [27] E.M. Henley, G. Krein, and A.G. Williams, Phys. Lett. **B 281** (1992) 178.
- [28] T. H. Bauer, R. D. Spital, D. R. Yennie, and F. M. Pipkin, Rev. Mod. Phys. **50**, 261 (1978); *ibid* **51**, 407(E) (1979); D. G. Cassel *et al.*, Phys. Rev. **D24**, 2787 (1981).
- [29] P. Joos *et al.*, Nucl. Phys. **B122**, 365 (1977).
- [30] A. Donnachie and P.V. Landshoff, Phys. Lett. **B 185**, 403 (1987).

- [31] P.V. Landshoff and O. Nachtmann, *Z. Phys.* **C35**, 405 (1987); A. Donnachie and P.V. Landshoff, *Nucl. Phys.* **B311**, 509 (1988/1989); *Phys. Lett.* **B 296**, 227 (1992); J.R. Cudell, *Nucl. Phys.* **B315**, 459 (1993); S.V. Goloskokov, *Phys. Lett.* **B315**, 459 (1993); J.-M. Laget and R. Mendez-Galain, *Nucl. Phys.* **A581**, 397 (1995).
- [32] M. Pichowsky and T.-S. H. Lee, *Phys. Rev.* **D56**, 1644 (1997).
- [33] A. I. Titov, Y. Oh, and S. N. Yang, *Phys. Rev. Lett.* **79**, 1634 (1997); A. I. Titov, Y. Oh, S. N. Yang, and T. Morii, *Nucl.-th/9804043*.
- [34] H. Yukawa, *Phys. Rev.* **91**, 416 (1953); M.A. Markov, *Hyperons and K Mesons* (Fizmatgiz, Moscow, 1958); K. Fujimura, T. Kobayashi and M. Namiki, *Porg. Theor. Phys.* **44**, 193 (1970); *Prog. Theor. Phys.* **43**, 73 (1970); R.P. Feynman, M. Kisslinger and F. Ravndal, *Phys. Rev.* **D3**, 2706 (1971); R.G. Lipes, *Phys. Rev.* **D5**, 2849 (1972); Y.S. Kim and M.E. Noz, *Phys. Rev.* **D12**, 129 (1975); Y. Kizukuri, M. Namiki and K. Okano, *Prog. Theor. Phys.* **61**, 559 (1979); V.V. Burov, S.M. Dorkin, and V.K. Lukyanov and A.I. Titov, *Z. Phys.* **A 306**, 149 (1982).
- [35] A.I. Titov *et al.*, in preparation.
- [36] A. S. Raskin and T. W. Donnelly, *Ann. Phys.* **191**, 78 (1989).
- [37] T.-S. H. Lee and A. Titov, in progress
- [38] Jlab experiment E93-031, spokespersons: L.M. Laget, M. Anghinolfi, C. Marchand.
- [39] Jlab experiment E93-022, spokespersons: H. Funsten, P. Rubin and E.S. Smith.
- [40] Jlab proposal PR96-x, spokespersons: D.J. Tedeschi, J.A. Mueller, P.L. Cole.
- [41] L. Ahrens *et al.*, *Phys. Rev. Lett.* **31**, 131 (1973); *ibid* *Phys. Rev.* **D9**, 1894 (1974).
- [42] Jlab experiment E94-010, Spokespersons: G. Cates and Z.-E. Meziani.
- [43] Jlab experiment E89-033, Spokespersons: C. Chang, C. Glashausser, S. Nanda, P. Rutt.
- [44] D.C. Fries *et al.*, *Nucl. Phys.* **B143**, 408 (1978); D.P. Barber *et al.*, *Z. Phys.* **C12**, 1 (1982).
- [45] K. Wacker, DESY internal report DESY F1-76/04, 1976.
- [46] M.W.McNaughton *et al.*, *NIM*, **A241** 435 (1985).

FIGURES

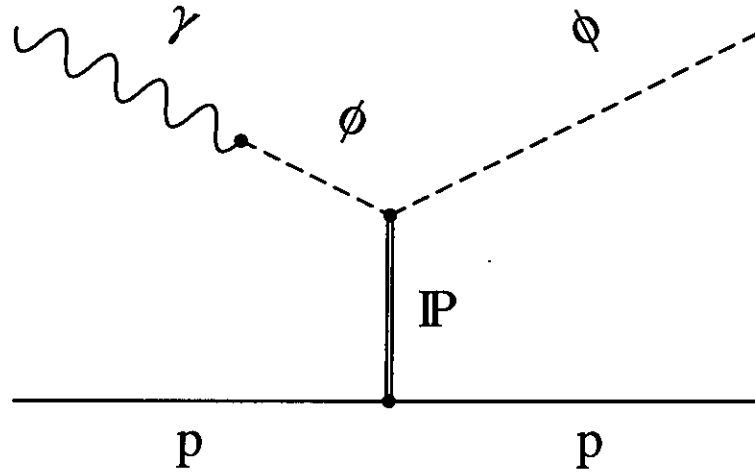


FIG. 1. Diffractive ϕ meson production within the vector-meson-dominance model by means of Pomeron exchange.

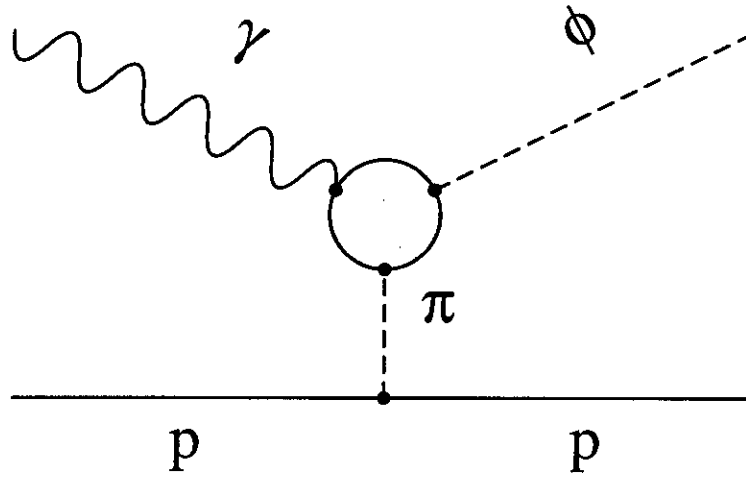


FIG. 2. One pion exchange process in the ϕ photoproduction.

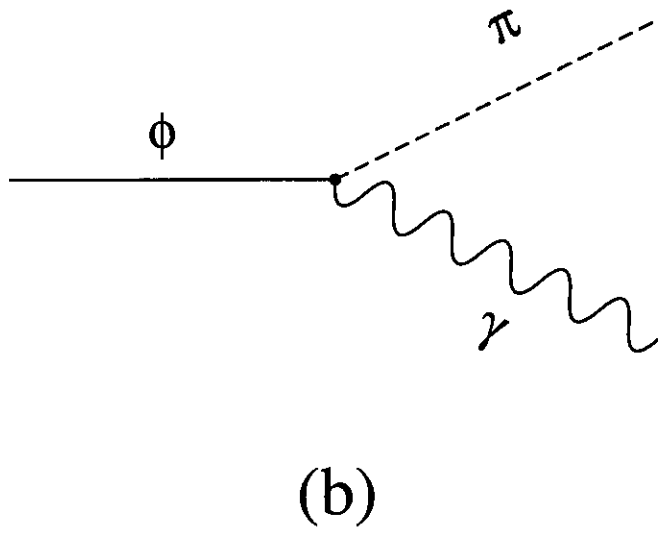
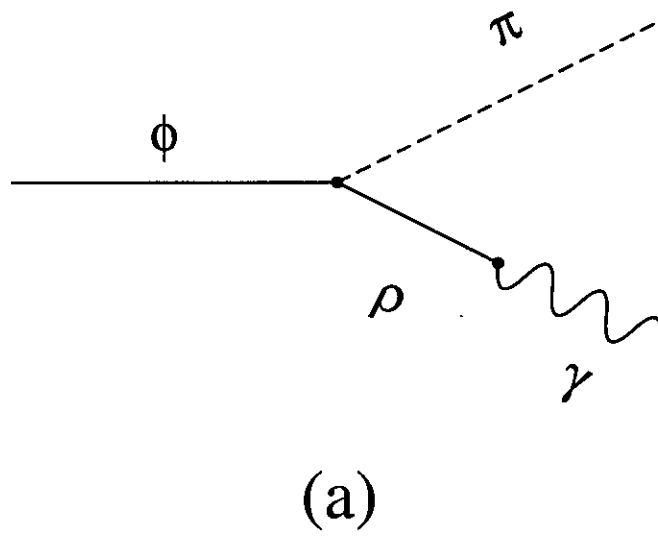
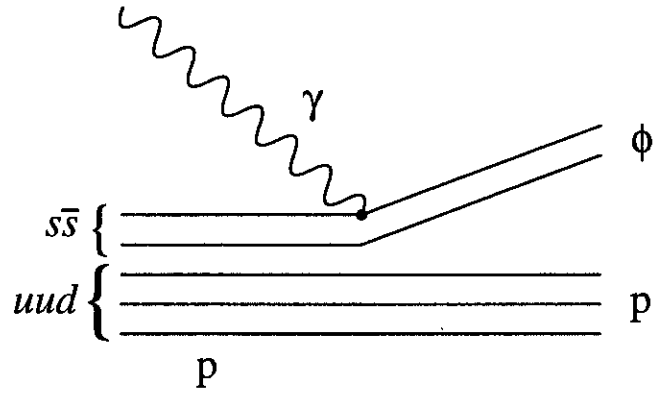
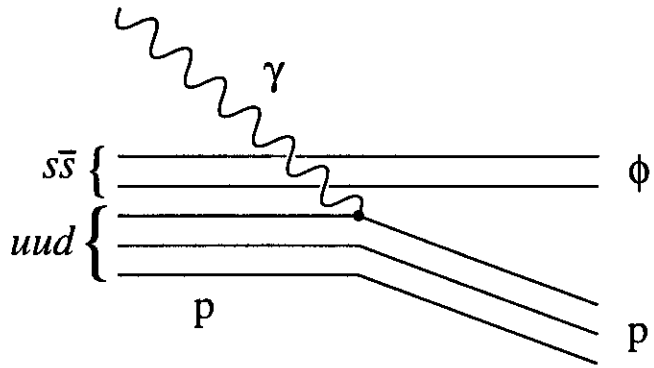


FIG. 3. Two possible mechanisms of $\phi \rightarrow \gamma\pi$ decay.



(a)



(b)

FIG. 4. (a) $s\bar{s}$ -knockout and (b) uud -knockout contributions to ϕ meson photoproduction.

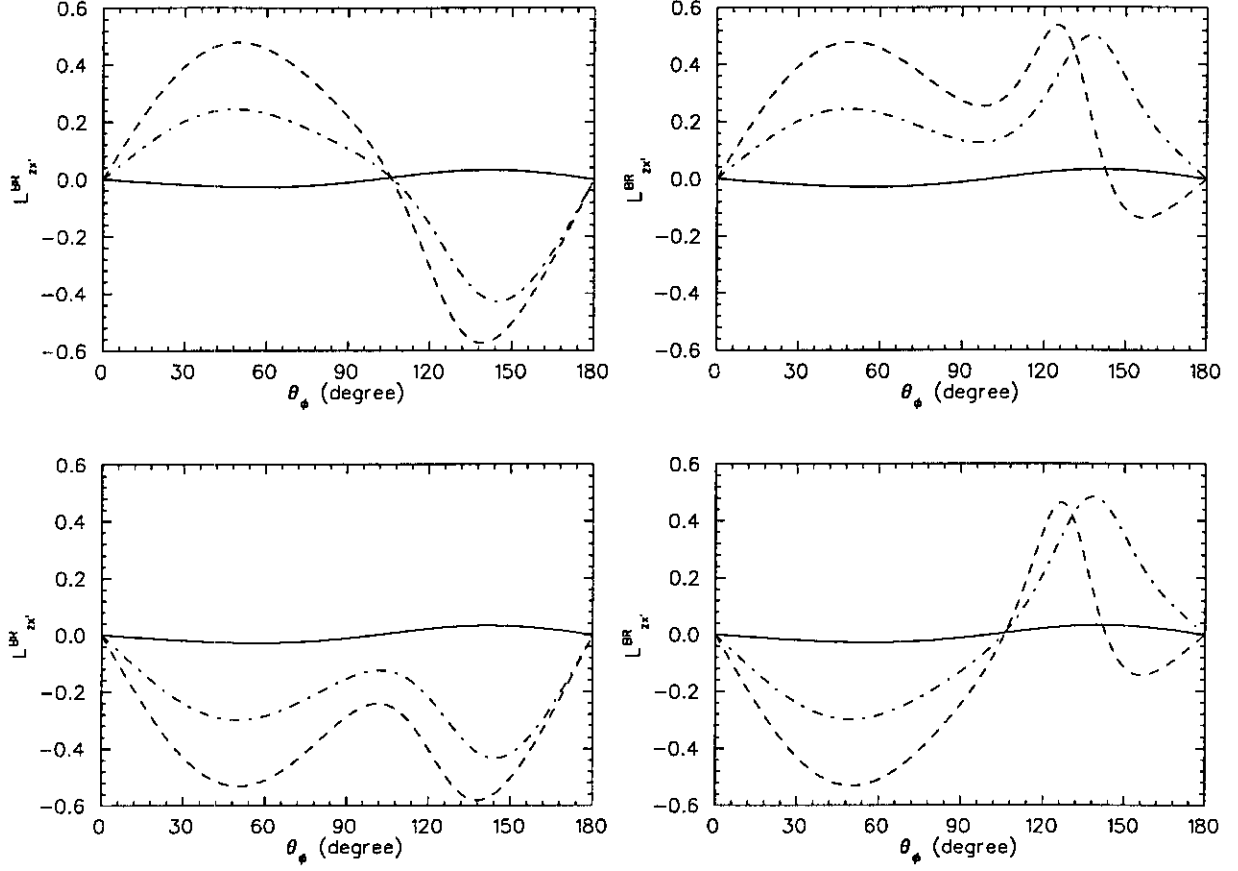


FIG. 5. Longitudinal beam-recoil asymmetry as a function of ϕ_{cm} calculated by Titov, Oh and Yang for photoproduction of ϕ mesons from protons. The solid, dash-dotted and dashed lines correspond to VMD+OPE, 0.25% $\bar{s}s$ probability, and 1% $\bar{s}s$, respectively. The four different panels correspond to four different phase combinations in the mixing of the two spin configurations of $\bar{s}s$.

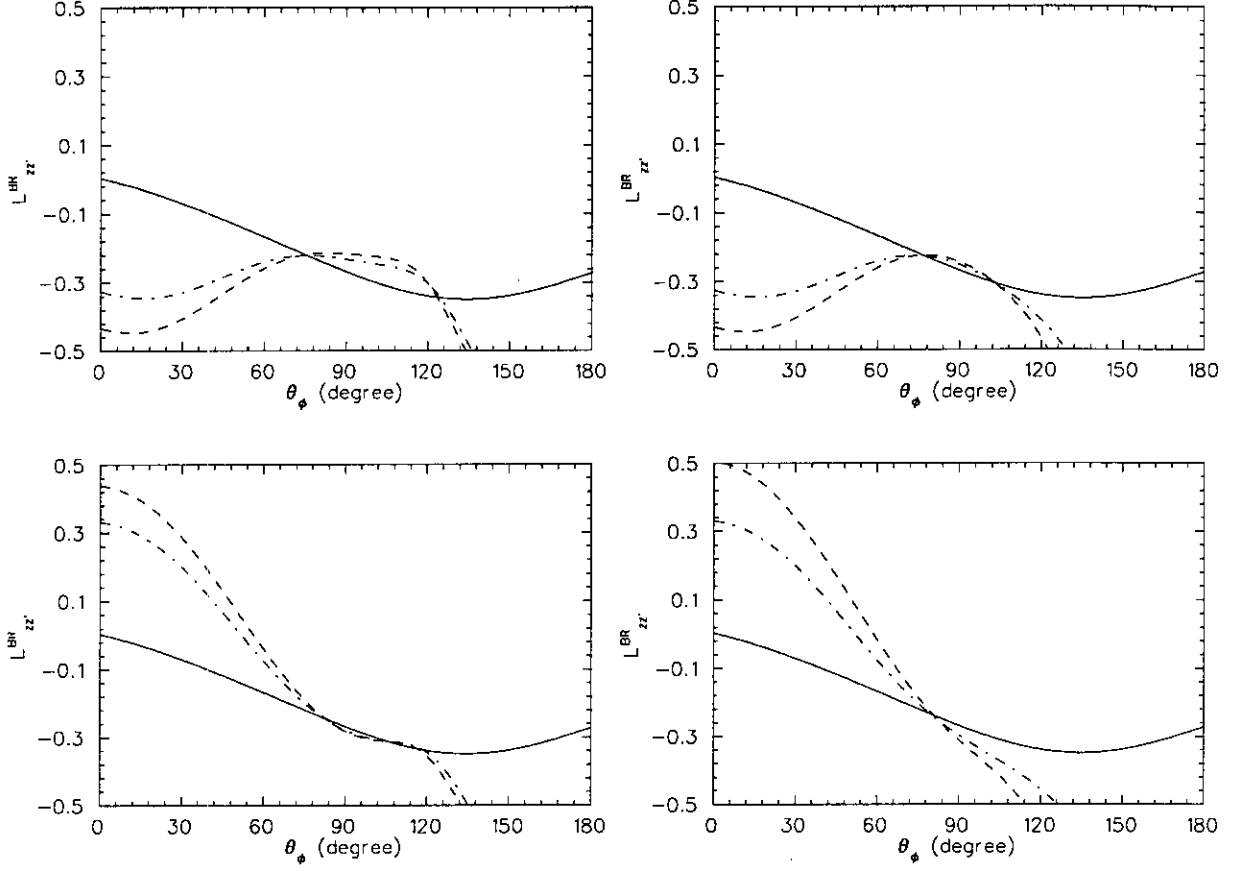


FIG. 7. The beam-recoil asymmetry $L_{zz'}^{BR}$ from electroproduction of ϕ meson as a function of ϕ_{cm} calculated by Titov *et al.* at a $|Q^2| = 0.135$ (GeV/c) 2 (see text). The solid, dash-dotted and dashed lines correspond to VMD+OPE (no strangeness), 1.0% $\bar{s}s$ probability, and 2.0% $\bar{s}s$, respectively. The four different panels correspond to four different phase combinations in the mixing of the two spin configurations of $\bar{s}s$.

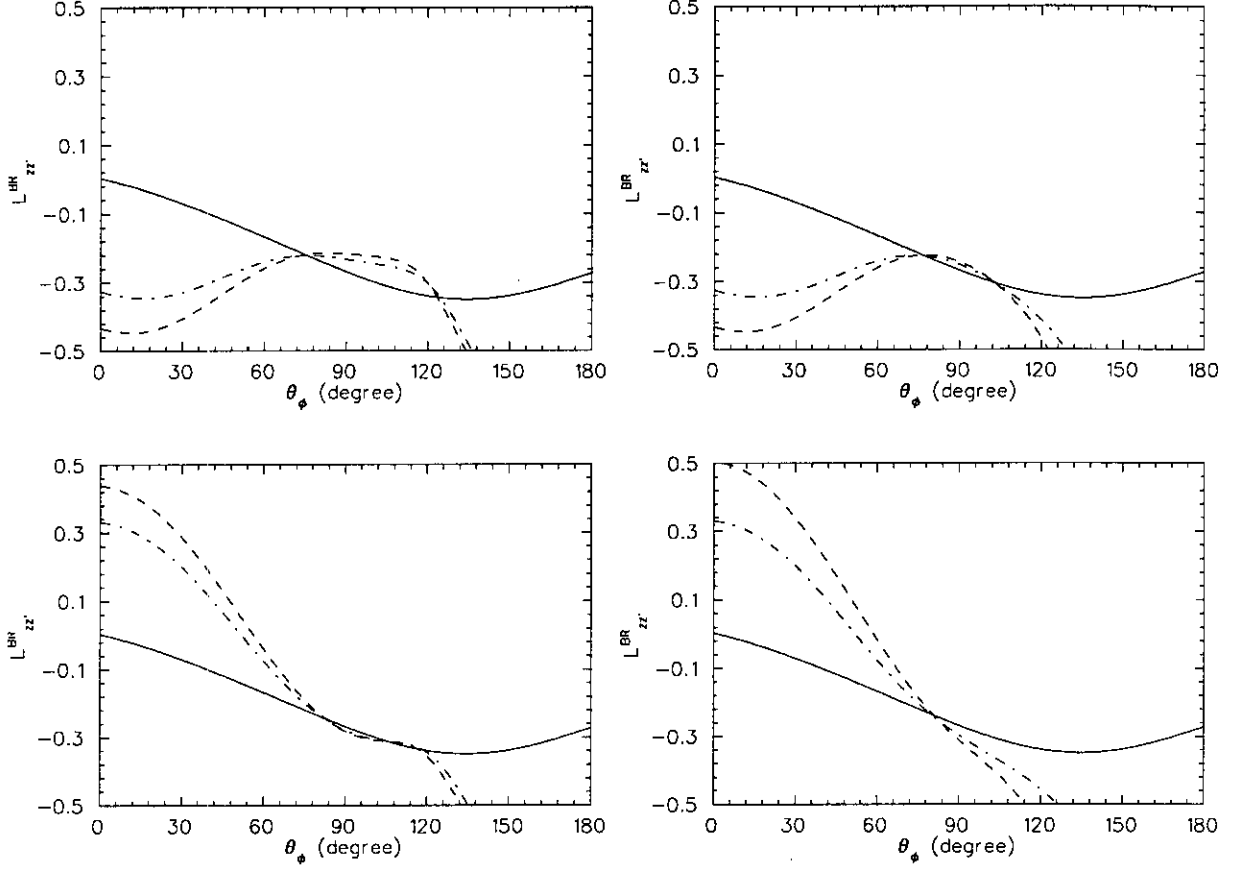


FIG. 7. The beam-recoil asymmetry $L_{zz'}^{BR}$ from electroproduction of ϕ meson as a function of ϕ_{cm} calculated by Titov *et al.* at a $|Q^2| = 0.135$ (GeV/c) 2 (see text). The solid, dash-dotted and dashed lines correspond to VMD+OPE (no strangeness), 1.0% $\bar{s}s$ probability, and 2.0% $\bar{s}s$, respectively. The four different panels correspond to four different phase combinations in the mixing of the two spin configurations of $\bar{s}s$.

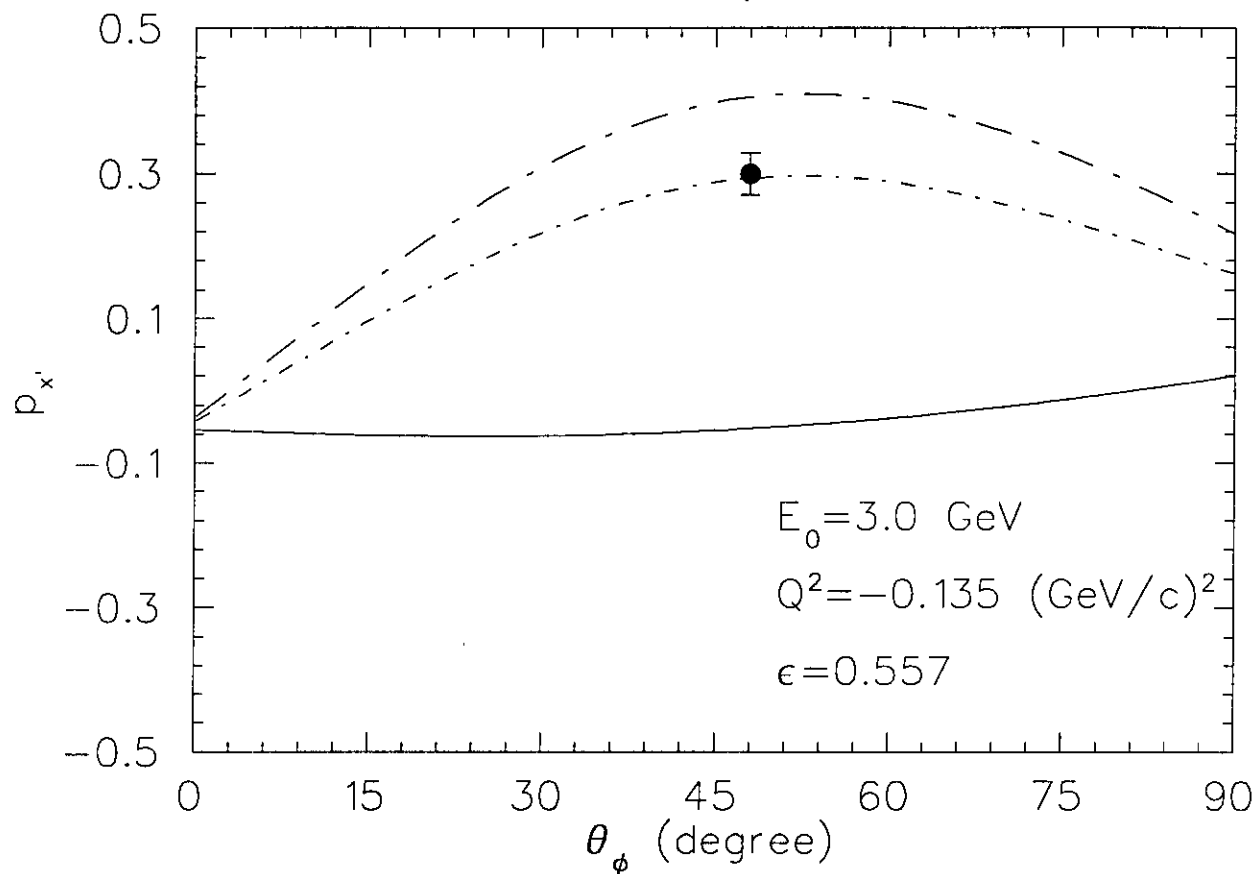


FIG. 8. Proposed measurement of P_x' from FPP at kinematic setting of this experiment is shown with the projected statistical uncertainty only, which dominates the overall uncertainty of the measurement. The solid, long dash-dotted and dash-dotted lines correspond to VMD+OPE (no strangeness), 2.0% $\bar{s}s$ probability, and 1% $\bar{s}s$, respectively. The phase combination of (+1,+1) for the spin configurations of $\bar{s}s$ is shown only for simplicity.

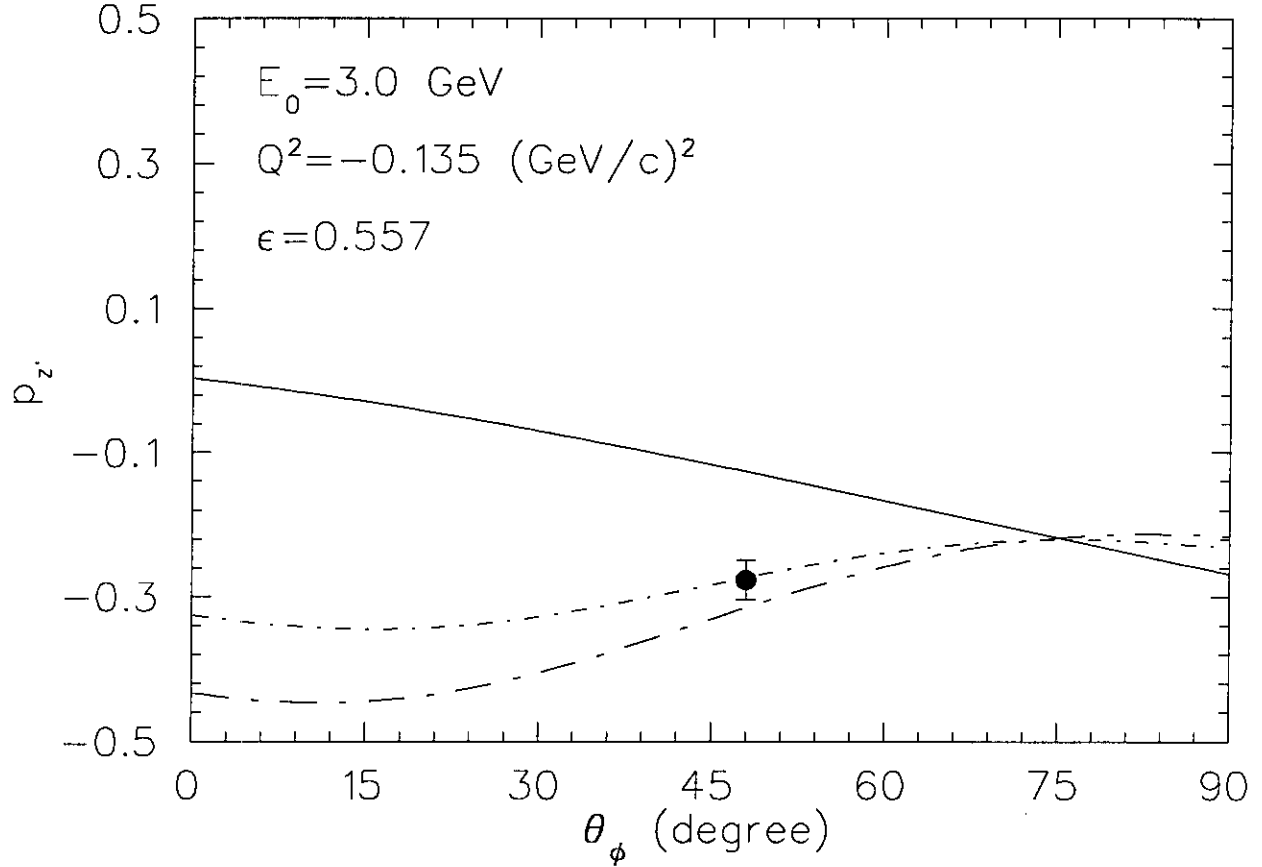


FIG. 9. Proposed measurement of P_z from FPP at kinematic setting of this experiment is shown with the projected statistical uncertainty only, which dominates the overall uncertainty of the measurement. The solid, long dash-dotted and dash-dotted lines correspond to VMD+OPE (no strangeness), 2.0% $\bar{s}s$ probability, and 1% $\bar{s}s$, respectively. The phase combination of (+1,+1) for the spin configurations of $\bar{s}s$ is shown only for simplicity.

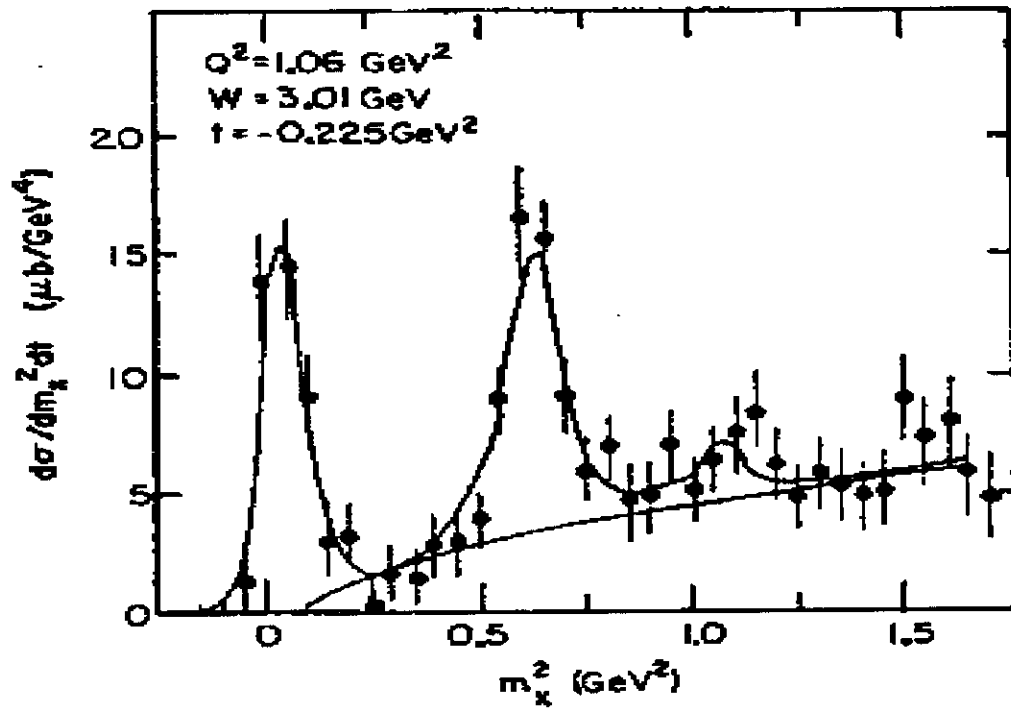


FIG. 10. Sample missing-mass-squared spectrum for $\gamma^* + p \rightarrow p + X$ from the earlier work by Ahrens *et al.*.

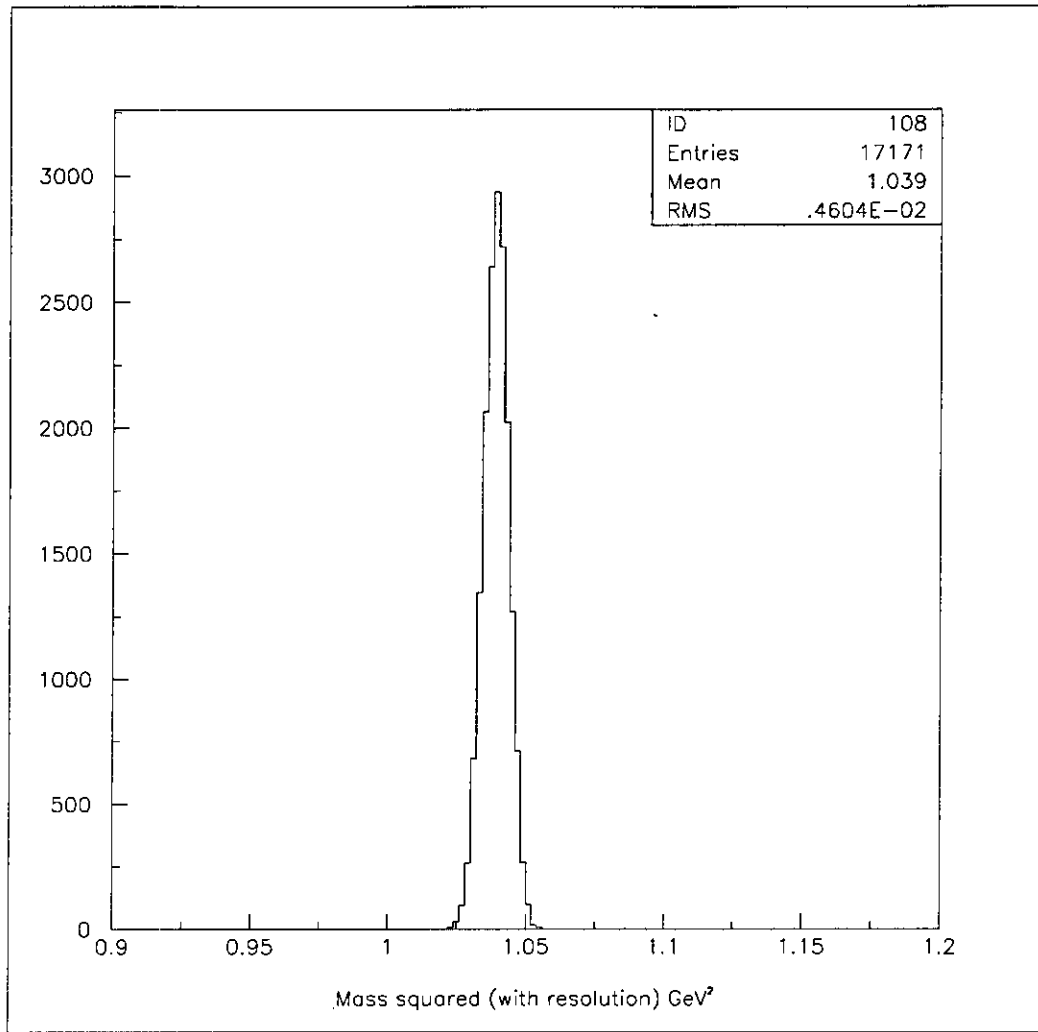


FIG. 11. The simulated missing mass squared resolution at the kinematic setting of this experiment from reconstruction only for ϕ detection.

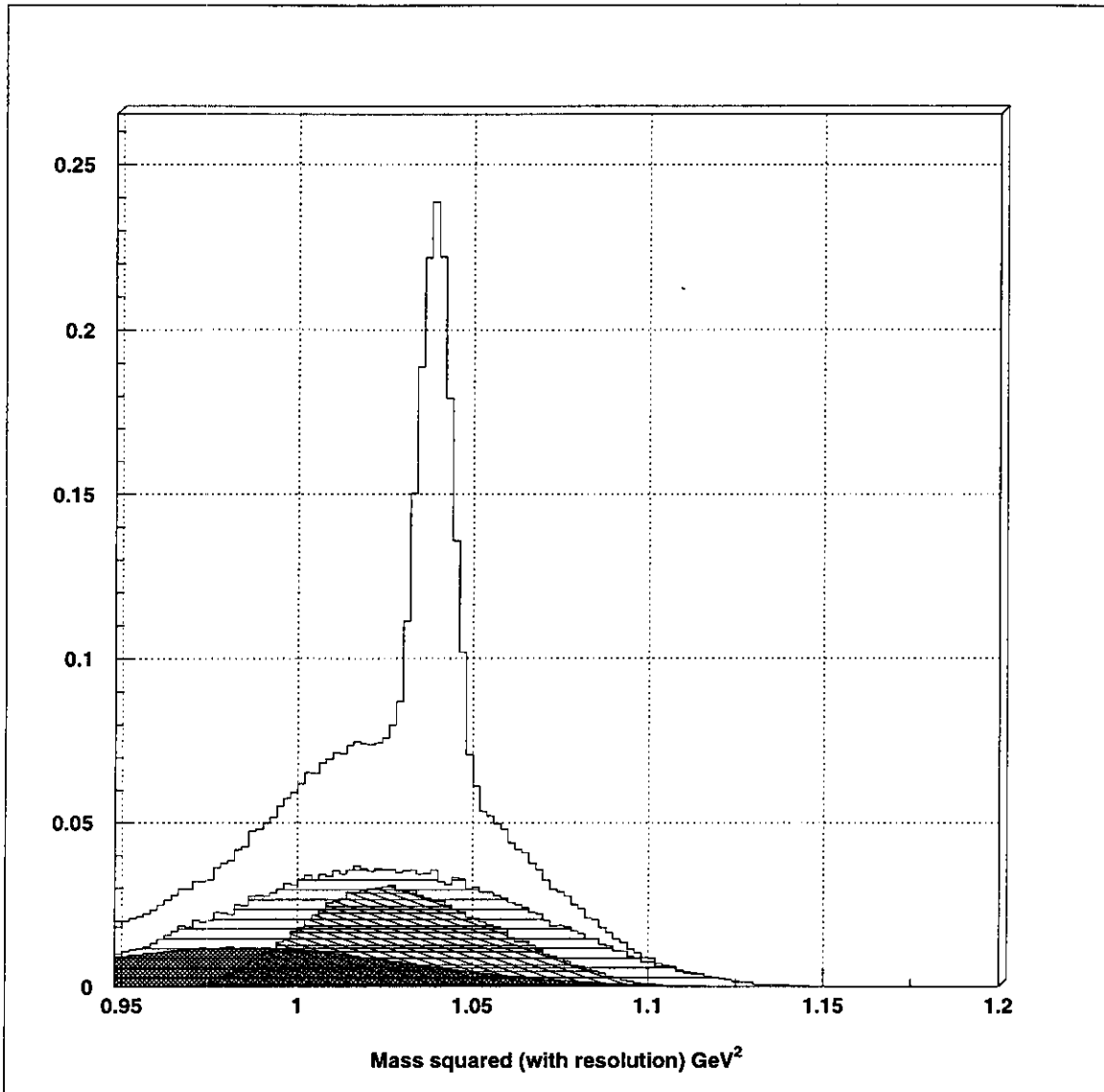


FIG. 12. The simulated experimental missing mass spectrum at the 5 GeV kinematics. The accidental background is shown as the vertical hatches, the non-resonant K^+K^- and the $\pi^+\pi^-$ backgrounds are shown as the slanted and horizontal hatches, respectively.